

Identification, Synthesis, and Characterization of Novel Baricitinib Impurities

Guruswamy Vaddamanu, Anandarup Goswami,* N. Ravi Sekhar Reddy, Katam Reddy Vinod Kumar Reddy, and Naveen Mulakayala*



Cite This: *ACS Omega* 2023, 8, 9583–9591



Read Online

ACCESS |



Metrics & More

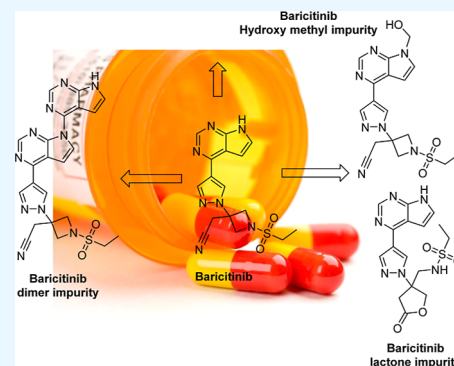


Article Recommendations



Supporting Information

ABSTRACT: Baricitinib is a novel active pharmaceutical ingredient used in the treatment of rheumatoid arthritis, and it acts as an inhibitor of Janus kinase. During the synthesis of baricitinib, three unknown impurities were identified in several batches between 0.10 and 0.15% using high-performance liquid chromatography. The unknown compounds were isolated and identified as *N*-((3-(4-(7*H*-pyrrolo[2,3-*d*]pyrimidin-4-yl)-1*H*-pyrazol-1-yl)-5-oxotetrahydrofuran-3-yl)methyl)ethane sulfonamide (lactone impurity, BCL), 2-(3-(4-(7*H*-[4,7'-bipyrrolo[2,3-*d*]pyrimidin]-4'-yl)-1*H*-pyrazol-1-yl)-1-(ethylsulfonyl)azetidin-3-yl)acetonitrile (dimer impurity, BCD), and 2-(1-(ethylsulfonyl)-3-(4-(7-(hydroxymethyl)-7*H*-pyrrolo[2,3-*d*]pyrimidin-4-yl)-1*H*-pyrazol-1-yl)azetidin-3-yl) acetonitrile (hydroxymethyl, BHM). These compounds were synthesized and confirmed against the isolated samples. The structures of all the three impurities were confirmed by extensive analysis of ¹H NMR, ¹³C NMR, and mass spectrometry. The lactone impurity formation was explained by a plausible mechanism. The outcome of this study was very useful for scientists working in process as well as in formulation development. To synthesize highly pure baricitinib drug substance, these impurities can be used as reference standards due to their potential importance.



1. INTRODUCTION

Baricitinib **1** (Olmiant), chemically known as 2-[1-ethylsulfonyl-3-[4-(7*H*-pyrrolo[2,3-*d*]pyrimidin-4-yl)pyrazol-1-yl]-

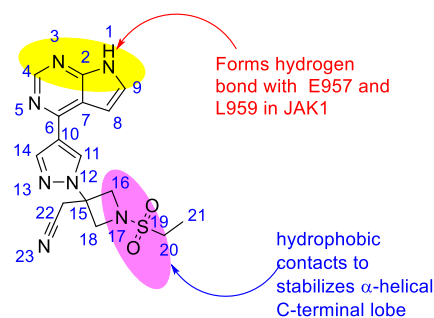


Figure 1. Chemical structure of baricitinib.

azetidin-3-yl] acetonitrile [Figure 1], is used in the treatment of rheumatoid arthritis (RA), graft-versus-host disease, myelofibrosis, and COVID-19.^{1–3} RA is a disease whose occurrence is seen to be increasing every year. Currently, 14 million adults are affected by RA worldwide. Baricitinib has been in use for severely affected patients with RA having less response against TNF antagonists. It inhibits the Janus kinase (JAK) enzyme by blocking JAK1 and JAK2 subtype enzymes.

Several clinical studies showed that baricitinib is effective in the treatment of severe atopic dermatitis and also in the treatment of alopecia areata.^{4,5} The United States Food and Drug Administration (USFDA) approved the use of baricitinib for RA in 2018 and COVID-19 in 2022 along with remdesivir.

Identification and control of impurities in drug substances and drug products are very critical for their safety assessment. These impurities affect the drug efficacy, quality, and safety. The maximum daily dosage of baricitinib in RA patients is 4 mg.⁶

International Council for Harmonization (ICH) tripartite guidelines suggest that the reporting threshold is 0.05% and the identification threshold is 0.10% for impurities in new drug substances for a maximum daily dose of ≤2 g/day.⁷ The efficacy and safety of the drug mainly depend on the impurities present in the drug substance. The toxicology of the drug mainly depends on the impurities present in the drug substance. Thus, identification and isolation of these impurities formed during the synthesis of active pharmaceutical

Received: January 6, 2023

Accepted: February 10, 2023

Published: March 2, 2023



Scheme 1. Chemical Synthesis of Baricitinib

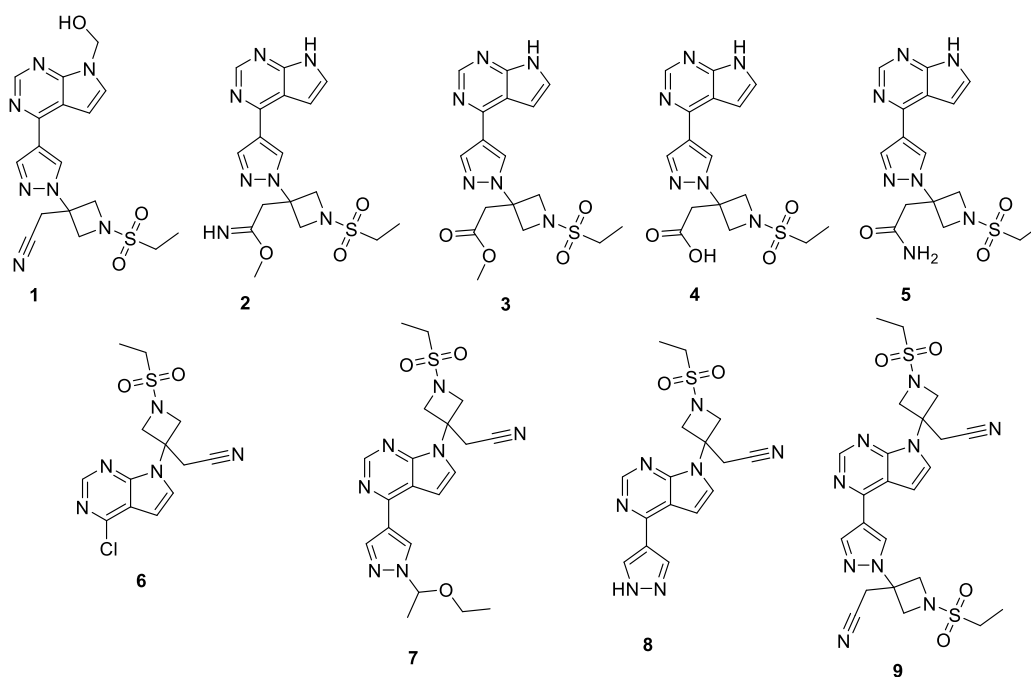
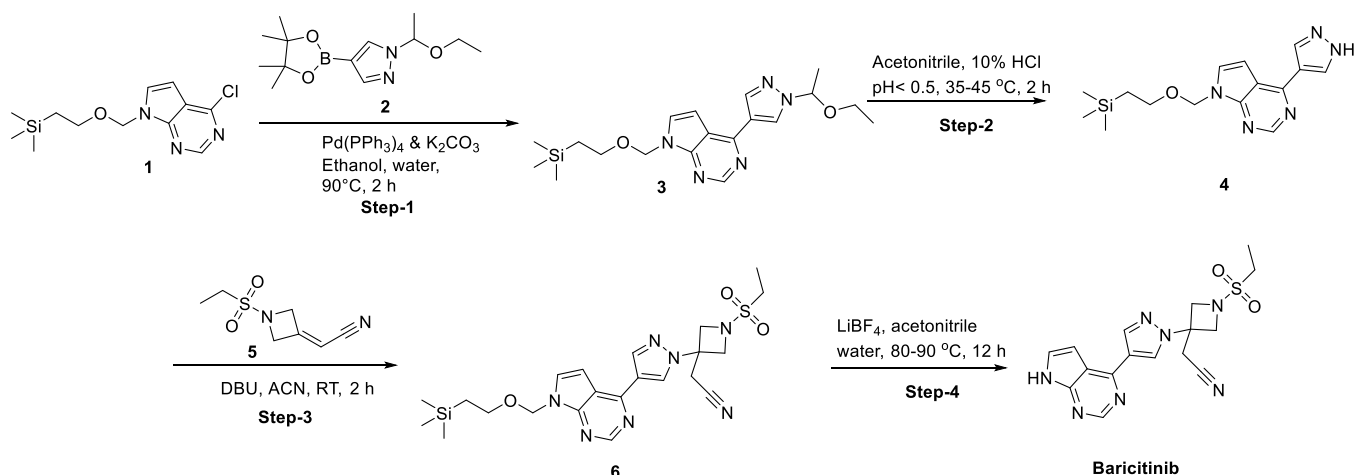


Figure 2. Chemical structures of reported baricitinib impurities.

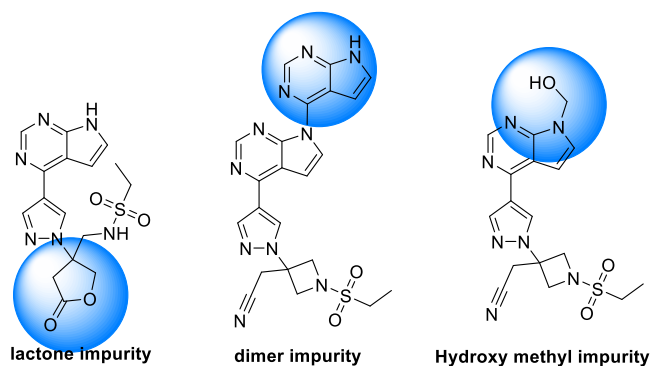


Figure 3. Three new impurities identified during the process development of baricitinib.

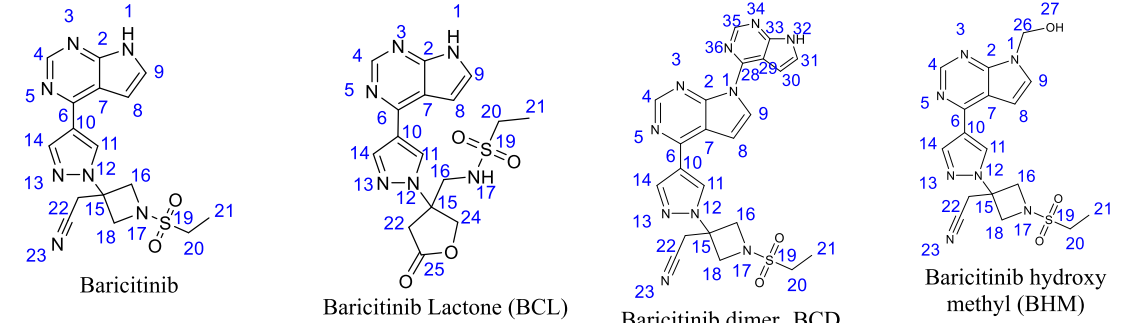
ingredient (API) products are very important to address the key requirements for the regulatory agency approval. Due to

very little literature availability, synthesis of these impurities becomes a challenging task for the manufacturers.

Thus, identification of impurities in a drug substance has a high impact on the efficacy of the drug. Due to this, there is a requirement of identification of unknown impurities in pharmaceutical substances.^{8–10} The formation of impurities and identifying their structures become a huge task in any drug substance which depends on the synthetic route and reaction conditions.

Baricitinib was synthesized following Scheme 1. In 2009, Rodgers et al. synthesized baricitinib by following Scheme 1.¹¹ Later, several researchers synthesized baricitinib using a similar procedure with slight modification in the protecting groups.

During the synthesis of baricitinib, several related impurities were identified in the literature (Figure 2).¹² Indeed, their synthesis and characterization of baricitinib impurities were limited. During the R&D synthesis and also pilot-scale synthesis, we observed three unknown impurities in the final product between 0.10 and 0.15% using high-performance

Table 1. ^1H NMR and ^{13}C NMR Assignment of BCL, BHM, and BCD Impurities


carbon number	^1H NMR ppm (multiplicity)	^{13}C NMR ppm	^1H NMR ppm (multiplicity)	^{13}C NMR ppm	^1H NMR ppm (multiplicity)	^{13}C NMR ppm	^1H NMR ppm (multiplicity)	^{13}C NMR ppm
1	12.16 (brs)	—	12.19 (brs)	—	—	—	—	—
2	—	152.2	—	152.07	—	151.88	—	150.80
3	—	—	—	—	—	—	—	—
4	8.71 (s)	150.91	8.69 (s)	150.82	8.80 (s)	150.60	8.80 (s)	150.76
5	—	—	—	—	—	—	—	—
6	—	149.36	—	149.63	—	147.56	—	149.47
7	—	113.05	—	112.93	—	115.00	—	113.51
8	7.09–7.10 (m)	99.55	7.09–7.10 (m)	99.98	6.83–6.84 (d, J = 3.6 Hz)	102.20	7.17–7.18 (d, J = 3.6 Hz)	—
9	7.63–7.64 (m)	126.95	7.59–7.60 (m)	126.70	7.51–7.52 (d, J = 4.0 Hz)	126.83	7.75–7.76 (d, J = 3.6 Hz)	129.72
10	—	122.22	—	121.75	—	121.57	—	121.71
11	8.93 (s)	129.62	8.84 (s)	129.68	8.89 (s)	129.10	8.97 (s)	129.87
12	—	—	—	—	—	—	—	—
13	—	—	—	—	—	—	—	—
14	8.49 (s)	139.92	8.39 (s)	139.26	8.58(s)	140.15	8.51 (s)	139.99
15	—	56.06	—	67.77	—	56.22	—	56.15
16	4.60–4.62 (d, J = 9.2 Hz)	58.55	3.62–3.72 (m)	47.74	4.63–4.65 (d, J = 9.2 Hz)	58.55	4.60–4.62 (d, J = 9.2 Hz)	58.56
17	—	—	7.66–7.69 (t, J = 6.8 Hz)	—	—	—	—	—
18	4.23–4.26 (d, J = 9.6 Hz)	58.55	—	—	4.26–4.28 (d, J = 9.2 Hz)	58.55	4.24–4.26 (d, J = 9.2 Hz)	66.48
19	—	—	—	—	—	—	—	—
20	3.22–3.27 (q)	43.27	2.91–2.97 (q)	45.78	3.23–3.29 (q)	43.34	3.22–3.27 (q)	43.35
21	1.23–1.27 (t, 7.2 Hz)	7.44	1.11–1.14 (t, J = 7.2 Hz)	7.90	1.24–1.28 (t, J = 7.2 Hz)	7.47	1.23–1.27 (t, J = 7.2 Hz)	7.46
22	3.70 (s)	26.84	3.27–3.36 (d, J = 18.0 Hz)	37.43	3.73 (s)	26.92	3.70 (s)	26.86
22'	—	—	3.47–3.51 (d, J = 14.8 Hz)	—	—	—	—	—
23	—	116.69	—	—	—	116.69	—	116.69
24	—	—	4.68–4.70 (d, J = 10.0 Hz)	73.34	—	—	—	—
24'	—	—	4.82–4.85 (d, J = 10.0 Hz)	—	—	—	—	—
25	—	—	—	174.09	—	—	—	—
26	—	—	—	—	—	—	5.64 (s)	100.25
27	—	—	—	—	—	—	6.65 (brs)	—
28	—	—	—	—	—	153.89	—	—
29	—	—	—	—	—	130.13	—	—
30	—	—	—	—	8.30–8.31 (d, J = 4.0 Hz)	110.17	—	—
31	—	—	—	—	7.66–7.67 (d, J = 3.2 Hz)	103.18	—	—
32	—	—	—	—	12.45 (brs)	—	—	—
33	—	—	—	—	—	150.46	—	—
34	—	—	—	—	—	—	—	—
35	—	—	—	—	9.06 (s)	151.18	—	—
36	—	—	—	—	—	—	—	—

liquid chromatography (HPLC). These impurities after liquid chromatography–mass spectrometry (LC–MS) analysis were identified as *N*-(3-(4-(7*H*-pyrrolo[2,3-*d*]pyrimidin-4-yl)-1*H*-pyrazol-1-yl)-5-oxotetrahydrofuran-3-yl)methyl)ethane sulfonamide (lactone impurity, BCL), 2-(3-(4-(7*H*-[4,7'-bipyrrolo[2,3-*d*]pyrimidin]-4'-yl)-1*H*-pyrazol-1-yl)-1-(ethylsulfonyl)-azetidin-3-yl)acetonitrile (dimer impurity, BCD), and 2-(1-(ethylsulfonyl)-3-(4-(7-(hydroxymethyl)-7*H*-pyrrolo[2,3-*d*]pyrimidin-4-yl)-1*H*-pyrazol-1-yl)azetidin-3-yl) acetonitrile (hydroxymethyl impurity, BHM) (Figure 3). Due to our interest toward the synthesis and identification of API impurities, we wish to report the synthesis and structural illustration of three major impurities of baricitinib obtained during the synthesis of baricitinib in this article.^{13–15}

2. EXPERIMENTAL SECTION

2.1. Chemicals and Reagents. The samples used in this study were synthesized in SVAK Life Sciences. BCL impurity, BCD impurity, and BHM impurity were synthesized and then purified using preparative HPLC if required. All the HPLC-grade solvents, NMR solvents, and reagents were procured from Merck Life Sciences, India.

2.2. HPLC (Analytical). A Waters (LC2695) HPLC system was used for the present study using a PDA-2996 detector set at 260 nm. Empower 2 software was used to process the HPLC data. The Epic C-18 (PerkinElmer, 250 mm × 4.6 mm, 5 μm) analytical column was used to perform the analysis. Mobile phase A was 10 mM ammonium acetate, and mobile phase B was methanol/acetonitrile (50:50, v/v). The linear gradient program was set as follows: T_{min}/B (mL/min): T 0/10; T15/90; T25/90; T26/10; T30/10. The flow rate was set at 1.0 mL/min, and the injection volume was 10 μL. The homogeneous mixture of HPLC-grade water and HPLC-grade methanol in the ratio 1:1 was used as a diluent for sample preparation.

2.3. Liquid Chromatography–Mass Spectroscopy. LC–MS analysis of the degraded sample of baricitinib was done on a Waters 2695 (Water Corporation) ACQUITY HPLC–MS system. The EPIC C18 column (4.6 × 150 mm, 3 μm) was used as an analytical column for chromatographic separation (Figures S28–S30). The wavelength of the UV detector was set at 260 nm. Mobile phase A consisted of 0.1% formic acid. Mobile phase B consisted of HPLC-grade acetonitrile. The flow rate was set at 0.8 mL per min, and the column oven temperature was set at 25 °C. The cone voltage was 30 V, and the capillary voltage was 3.5 kV. The source temperature was maintained at 120 °C. Nitrogen gas was used as both the desolvation and cone gases with flow rates of 350 L/h and 50 L/h, respectively. The linear gradient program was set as follows: T_{min}/B (%)—T 0/10; T15/90; T25/90; T26/10; T30/10.

2.4. HPLC (Preparative). Purification of BCL impurity was done from the enriched samples obtained from the reaction of baricitinib using the described procedure mentioned in Section 3.2. The required impurity peak (Figure S25) was isolated using the Waters 2545 preparative HPLC system equipped with the Phenomenex C18 column (250 × 20 mm, 10 μm), and the PDA2996 detector was set at 260 nm. Mass Lynx software was used to process the data. Ammonium bicarbonate, AR grade, in HPLC-grade water (pH 4.0; 0.02 M) with the pH adjusted with formic acid was used in mobile phase A, and HPLC-grade acetonitrile (100%) was used in mobile phase B. The flow rate was maintained at 15 mL/min,

and the run time was 40 min. The linear gradient program was set as follows: T_{min}/B (mL/min): T0/20; T5/30; T15/40; T20/50; T25/80; T35/90; T40/100. The BCL impurity obtained from the preparative HPLC fraction was extracted with 100 mL of MeOH–DCM (1:9), and the organic layer was concentrated to obtain BCL impurity as a pale yellow solid. The isolated sample was further used for its complete characterization.

3. RESULTS AND DISCUSSION

3.1. Identification of Unknown Impurity/Detection of Unknown Impurity.

To identify the unknown impurities

Table 2. DEPT and HMBC Assignment of BCL Impurity

carbon number	DEPT	HMBC	carbon number	DEPT	HMBC
1	—	—	15	C	H-16,22,22',24,24'
2	C	H-4,8,9	16	CH ₂	H-21,22,22',24,24'
3	—	—	17	—	—
4	CH	H-4,8,9,14	18	—	—
5	—	—	19	—	—
6	C	H-9,11,14	20	CH ₂	H-21
7	C	H-1,4,8,9,11	21	CH ₃	H-20
8	CH	H-1,4,9	22	CH ₂	H-16,22,22'
9	CH	H-1,8	22'	—	—
10	C	H-11,14	23	—	—
11	CH	H-14	24	CH ₂	H-16,22,22'
12	—	—	24'	—	—
13	—	—	25	C	H-22,22',24,24'
14	CH	H-11	—	—	—

which are formed during the synthesis of the baricitinib API, we recorded the LC–MS/MS spectrum of the unknown impurity. For BCL impurity, the mass obtained in the +ve mode was 391.05 and in the –ve mode was 389.06 (Figures S1 and S2). Dimer impurity in the +ve mode was 489.26 and in the –ve mode was 487.15 (Figures S13 and S14). The mass of the hydroxymethyl impurity in the +ve mode was 402.20 and that in the –ve mode was 400.34 (Figures S17 & S18). Based on the mass spectra and their fragmentation, we expected the unknown impurities as BCL, BCD, and BHM.

3.2. Synthesis of BCL Impurity. During the synthesis of baricitinib, the final step involves deprotection of the 2-(trimethylsilyl)ethoxymethyl acetal (SEM), acetyl, or *tert*-butoxycarbonyl (Boc) group present on the pyrrolo[2,3-*d*]pyrimidine core. Most of the literature involves usage of either acidic (or) basic conditions to deprotect the protecting groups. During this reaction, we observed the formation of 0.1 to 0.15% lactone impurity.

This led to an expectation that this lactone formation may be favorable either under acidic or basic conditions. The reaction standardization was done separately using acidic as well as basic conditions.

We performed the reactions using NaOH as a base at different concentrations. Sodium hydroxide in ethanol and water (9:1) was added to baricitinib in ethanol and treated at higher temperatures to obtain BCL in good yield. The maximum yield of BCL was observed by using NaOH (2 eq.) in ethanol and water (5 vol.) as a solvent at 80 °C for 48 h. The crude BCL was purified by using prep-HPLC to obtain the impurity with good purity. ¹H NMR and ¹³C NMR of BCL impurity data are presented in Table 1.

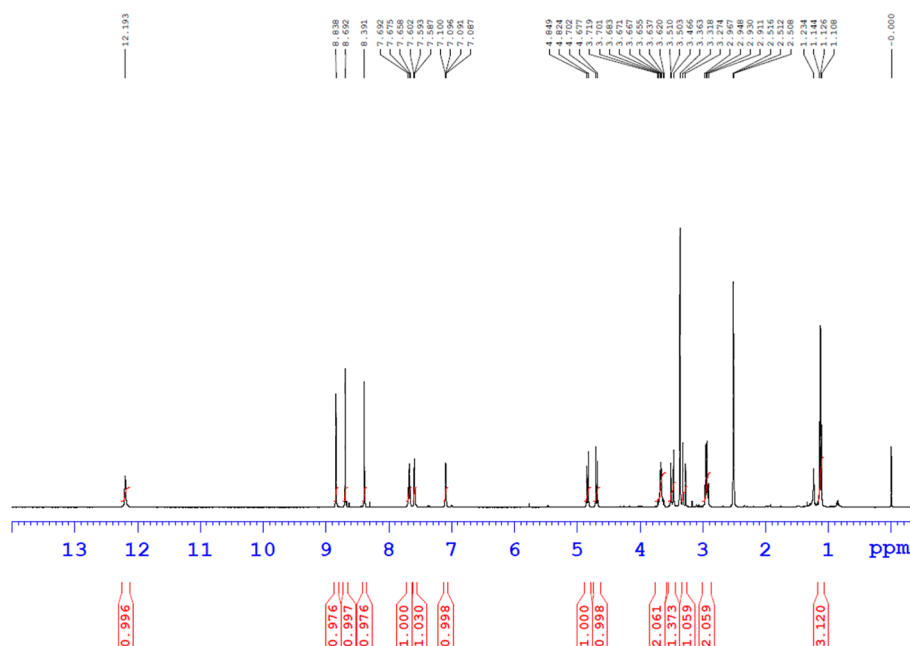


Figure 4. ^1H NMR spectrum of BCL impurity in $\text{DMSO}-d_6$.

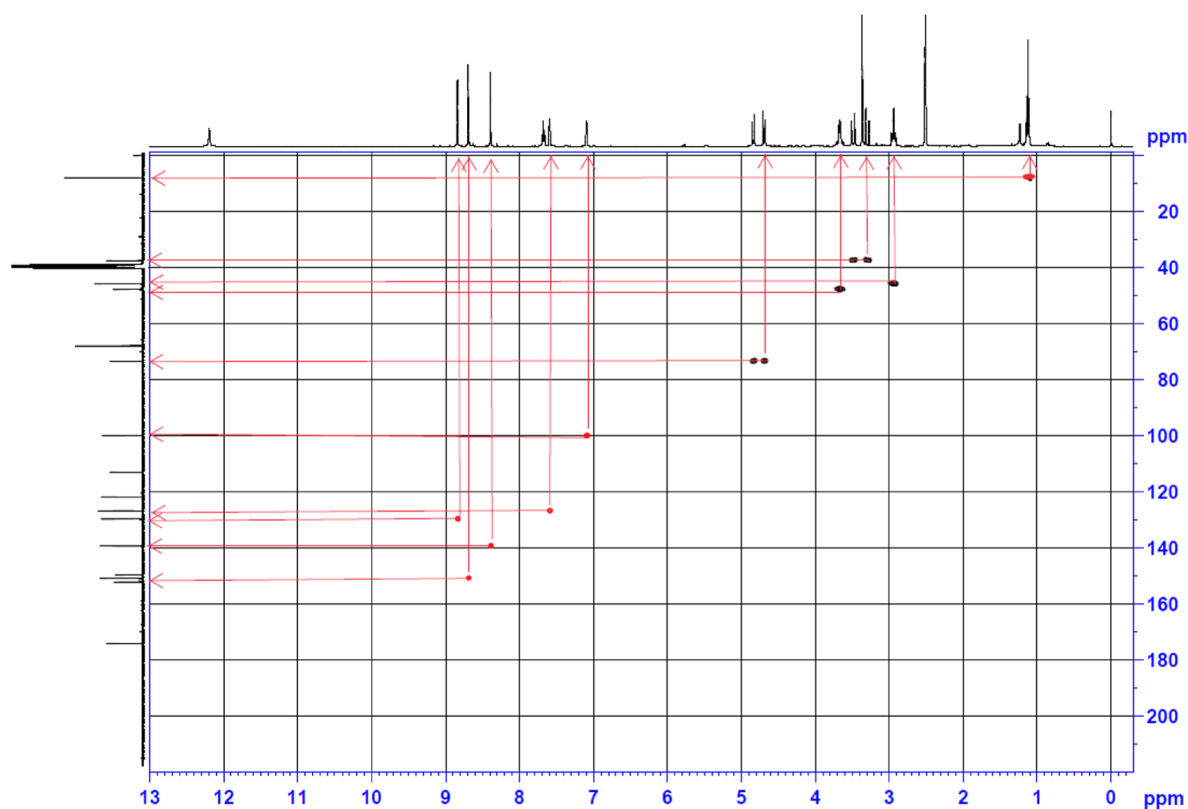


Figure 5. HSQC spectrum of BCL impurity in $\text{DMSO}-d_6$.

3.3. Synthesis of BCD Impurity. Baricitinib (1 g, 0.0027 moles) and 4-chloro-7*H*-pyrrolo[2,3-*d*]pyrimidine (0.62 g, 1.5 equiv) in 1,4-dioxane (15 mL) were degassed for 10 min, and Cs_2CO_3 (2.64 g, 3 equiv) and $\text{Pd}(\text{OAc})_2$ (0.12 g, 0.21 equiv) were added at room temperature. The contents were then stirred for 16 h at 100 °C. Reaction mass was concentrated, and the residue was taken in EtOAc (100 mL), filtered through the Celite pad, washed with ethyl acetate (20 mL), and the

filtrate was concentrated under reduced pressure to obtain crude (1.0 g). The crude compound was purified by silica gel (100–200 mesh, 10–12% MeOH in DCM) to afford 0.245 g of BCD as a pale brown solid. ^1H NMR and ^{13}C NMR data of BCD impurity are presented in Table 1.

3.4. Synthesis of BHM Impurity. 2-(1-(Ethylsulfonyl)-3-(4-(7-((2-(trimethylsilyl)ethoxy)methyl)-7*H*-pyrrolo[2,3-*d*]pyrimidin-4-yl)-1*H*-pyrazol-1-yl)azetidin-3-yl)acetonitrile (0.5

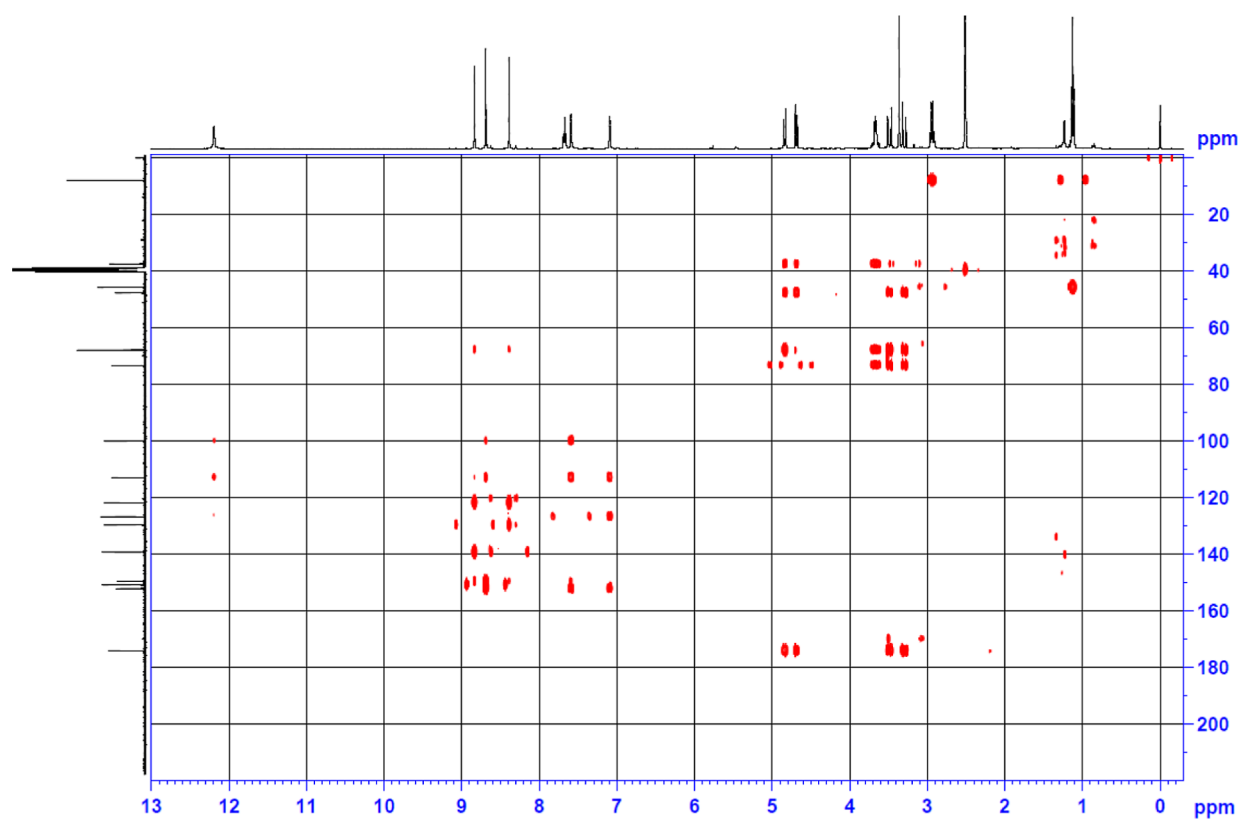


Figure 6. HMBC spectrum of BCL impurity in DMSO- d_6 .

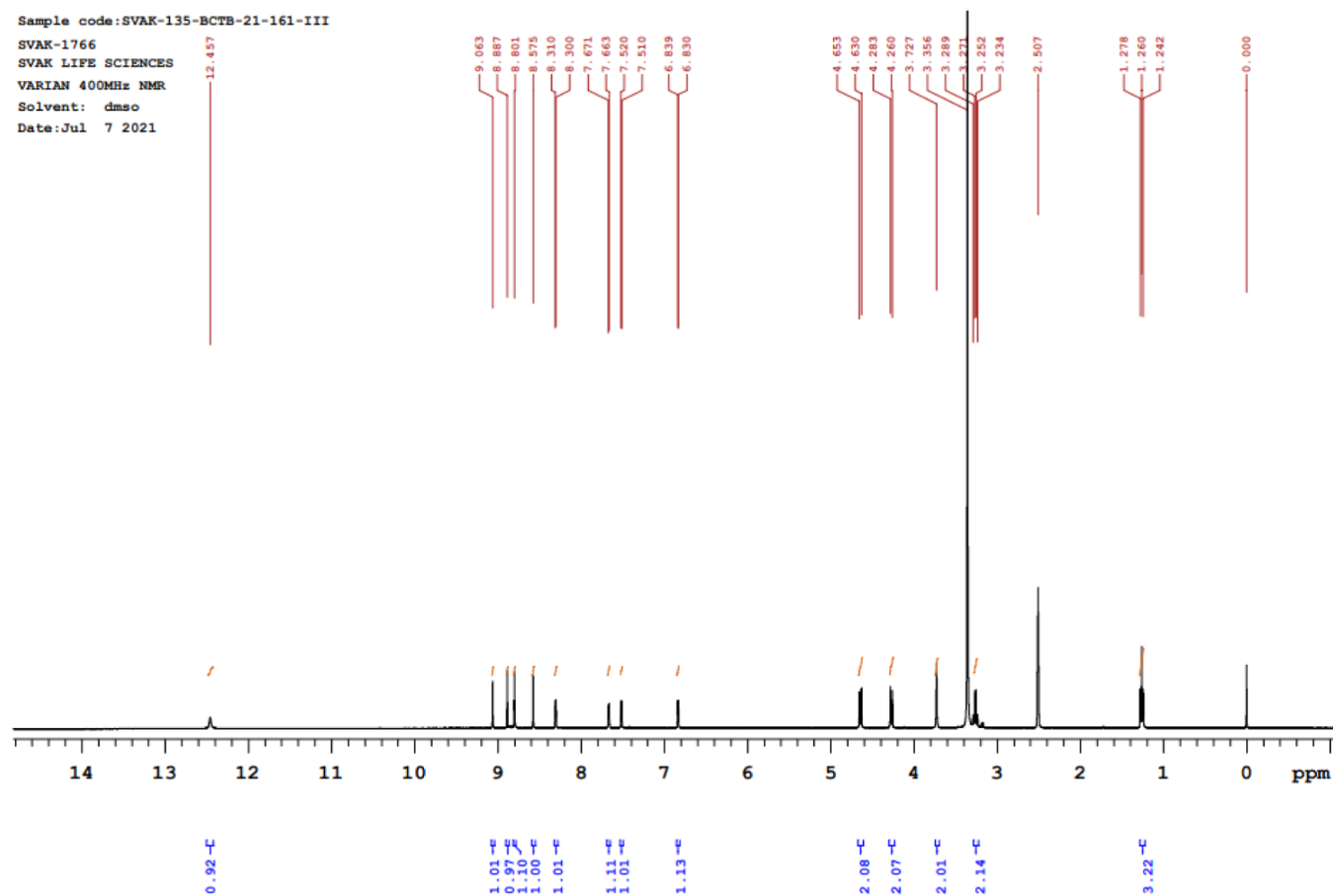


Figure 7. ^1H NMR spectrum of BCD impurity in DMSO- d_6 .

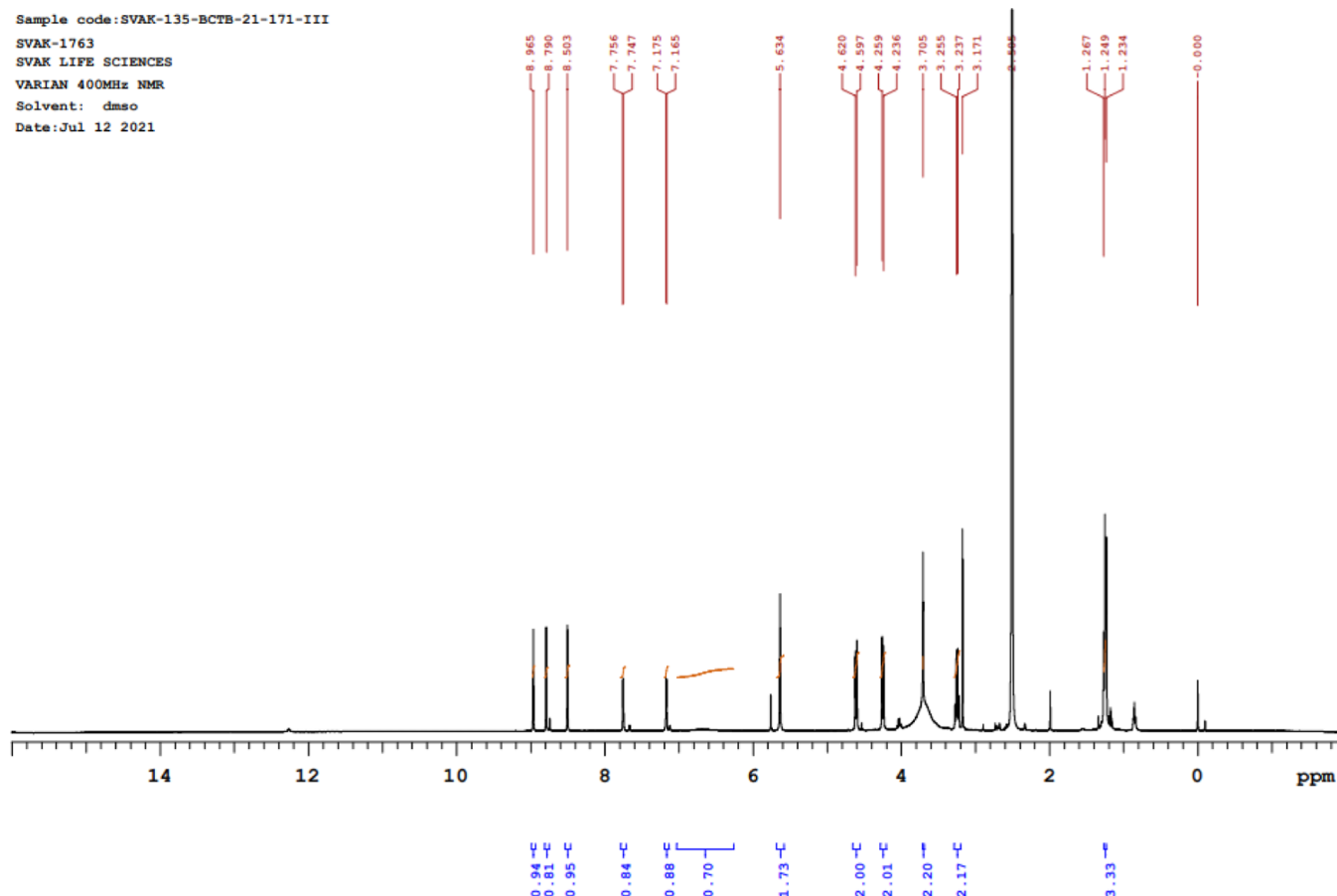


Figure 8. ^1H NMR spectrum of the BHM impurity in $\text{DMSO}-d_6$.

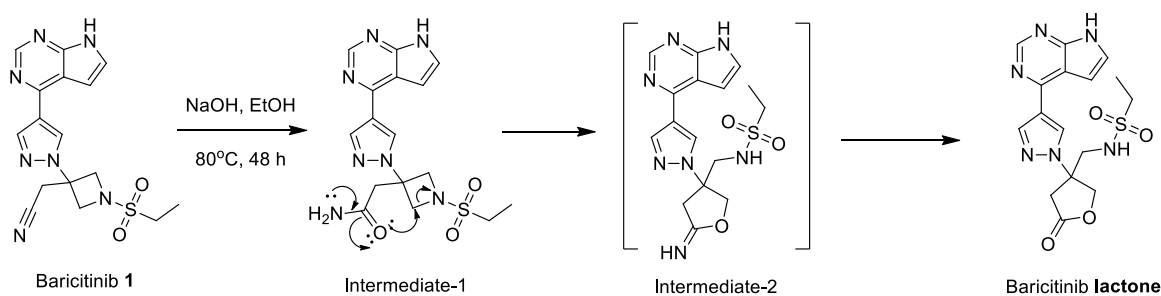


Figure 9. Plausible mechanism for the formation of BCL impurity.

g, 0.001 moles) was dissolved in chloroform (150 mL) and cooled to 10–15 °C. TFA (0.76 mL, 10 equiv) was added to the above reaction mixture at 10–15 °C. The reaction was kept at room temperature for 12 h. After completion of the starting material, the reaction mixture was evaporated and extracted with DCM (100 mL) to afford 250 mg of the pure compound as an off-white solid. ^1H NMR and ^{13}C NMR data of BHM impurity are presented in Table 1.

3.5. Structural Confirmation of the Three New Impurities. The structures of the three new impurities, *i.e.* BCL, BCD, and BHM, were confirmed by using several analytical methods such as ^1H NMR, ^{13}C NMR, and MS. For BCL, the structure was confirmed by analyzing with 2D NMR (COSY, HSQC, and HMBC). The NMR comparison of the BCL, BCD, and BHM impurities is shown in Table 1. The 2D NMR assignment of BCL is shown in Table 2.

The mass spectrum of the isolated impurity showed a base peak at m/z 391.05 in the +ve mode and a peak at 389.06 in the –ve mode, confirming the formation of BCL.

The ^1H NMR spectrum of baricitinib shows a peak at δ 12.19, indicating the presence of an –NH proton in the pyrrolo pyrimidine core, which is an exchangeable proton involved in the D_2O study. But, in ^1H NMR of the isolated impurity (Figure 4), we observed two exchangeable protons at δ 12.19 and δ 7.65–7.69 during the D_2O experiment. One of the peaks at δ 12.19 corresponds to the –NH proton which is present in the pyrrolo pyrimidine ring and is the same in both baricitinib and BCL. Another –NH proton which is a – SO_2NH proton at δ 7.65–7.69 having a triplet due to the presence of an adjacent methylene group (H-16) is also exchanged during the D_2O experiment in BCL.

In ^1H NMR spectra of baricitinib, H-22 protons are present at δ 3.70 corresponding to $-\text{CH}_2\text{CN}$ as a singlet peak, which

SVAK-1840
SVAK-145-21-BCL-002
1H DMSO-D6
12-02-2022

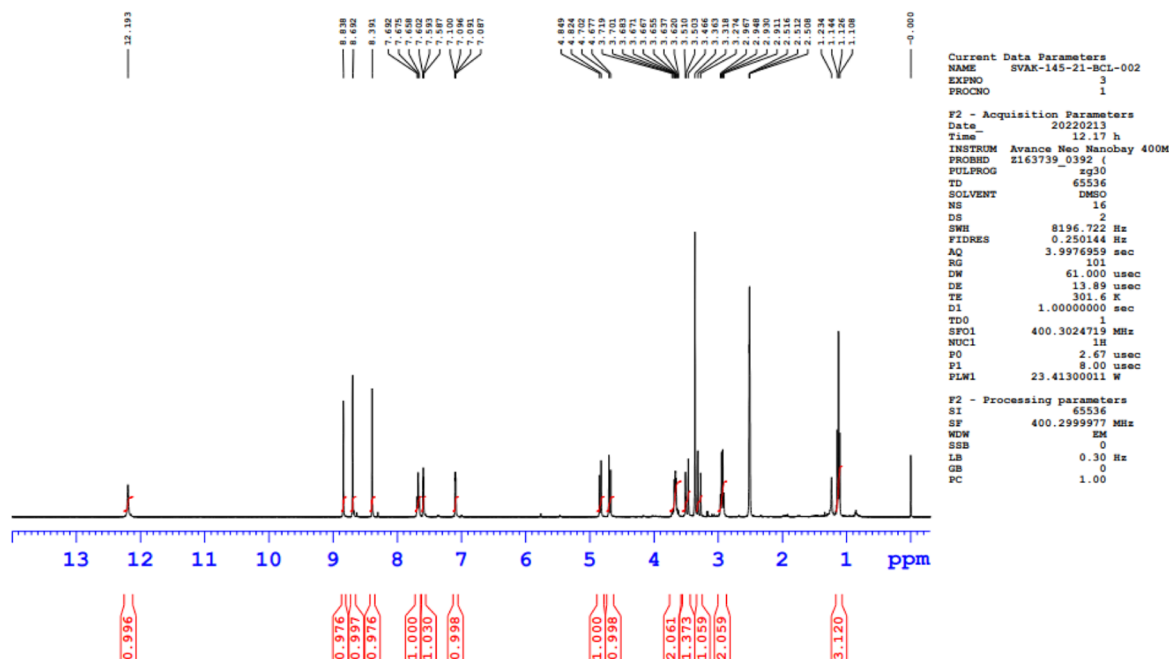


Figure 10. ^1H NMR spectrum of intermediate-1 in $\text{DMSO}-d_6$.

was shifted to upfield with two clear doublets at δ 3.27–3.36 and 3.47–3.51 in BCL impurity due to the formation of the lactone ring. In the ^{13}C NMR spectra of BCL impurity carbon at δ 174.09 corresponds to the $-\text{C}=\text{O}$ group of lactone ring. From the HSQC spectrum (Figure 5), it is evident that four $-\text{CH}_2$ protons (H-16, H-20, H-22, and H-24) are present in the BCL impurity.

The sequential correlation of H-16 and H-17 in ^1H - ^1H COSY confirmed that the opening of cyclic sulfonamide leads to the formation of lactone impurity. Furthermore, it was confirmed by HMBC, and the correlation between H-22, 22' (δ_{H} 3.27–3.36 and 3.47–3.51), H-24, 24' (δ_{H} 4.68–4.70 and 4.82–4.85), and H-16 (δ_{H} 3.62–3.72) with H-25 (δ_{C} 174.09) shows the formation of the lactone ring in the proposed structure (Figure 6).

After thorough analysis of all the spectral data, the structure of the isolated compound was assigned as BCL.

The mass spectrum of the synthesized BCD impurity showed a base peak at m/z 489.18 in the +ve mode and a peak at 487.15 in the -ve mode, showing the formation of BCD impurity, which matches with the mass spectrum of the isolated impurity. Furthermore, the compound was confirmed by using ^1H NMR and ^{13}C NMR. In the ^1H NMR spectrum (Figure 7), a peak at δ 12.45 indicates the presence of the -NH (H-32) proton in the pyrrolo pyrimidine core of the dimer compound which is distinct when compared with the baricitinib -NH proton in the pyrrolo pyrimidine core. Furthermore, there are few additional signals at δ 8.30–8.31 (d), δ 7.66–7.67 (d), and δ 9.06 (s) corresponding to the dimerized pyrrolo pyrimidine core unit. In the ^{13}C NMR spectrum also, we observed peaks at δ_{C} 150.46, 151.18, and 153.89 corresponding to C-28, C-33, and C-35 of the dimerized compounds, respectively. After in-depth analysis, it

was confirmed that the synthesized and isolated compounds were the same and was BCD.

To confirm the BHM impurity, we co-injected the isolated and synthesized samples. Both show the same peak in HPLC and the mass of 402.20 in the +ve mode and 400.34 in the -ve mode. In the ^1H NMR spectrum (Figure 8), two new peaks were observed at δ 5.64 (s) corresponding to the $-\text{CH}_2$ peak (H-26) and another broad singlet peak was observed at δ 6.65, corresponding to the hydroxy peak (27-OH). Also, the $-\text{NH}$ proton of the pyrrolo pyrimidine core disappeared, showing the formation of BHM impurity. In ^{13}C NMR, an additional peak at δ_{C} 100.25 shows the presence of $-\text{CH}_2$ carbon (C-26), and also, the change in the chemical shift of C-2 and C-9 carbons confirms the formation of the required impurity. All these results confirm the isolated impurity as BHM impurity.

3.6. Plausible Formation Pathway of BCL Impurity. In all the reported impurities, BCL impurity was a critical impurity. That is why we have proposed the plausible mechanism for the formation of BCL impurity, which is presented in [Figure 9](#). The formation of BCL impurity was due to basic hydrolysis of cyanide to amide (intermediate-1) followed by an intramolecular rearrangement to get intermediate-2. Intermediate-2 on hydrolysis yields BCL impurity. We have isolated and characterized intermediate-1 using ^1H NMR ([Figure 10](#)). But, we were unsuccessful in isolating the intermediate-2 due to its instability.

Finally, we studied several conditions to control these impurities in the manufacturing process. For controlling BCL impurity, we maintained the reaction temperature below 20 °C during the deprotection process. To avoid the formation of BHM impurity, we maintained the reaction under 10 °C using boron trifluoride diethyl etherate as a reagent followed by workup with water and extraction with DCM. The DCM layer

was treated with aqueous ammonia for 24 h to get pure baricitinib.

4. CONCLUSIONS

In conclusion, it was confirmed that the three impurities isolated from different manufacturing batches of baricitinib are BCL, BHM, and BCD. All the impurities were confirmed by using different analytical techniques. All these impurities were conveniently prepared in the laboratory using available intermediates. These impurities are useful as reference materials in companies and research institutes. This will help the researchers to identify and control the formation of all the three impurities during their manufacturing process. This work would be of immense interest to researchers working in process and formulation development of the baricitinib API.

■ ASSOCIATED CONTENT

Supporting Information

The Supporting Information is available free of charge at <https://pubs.acs.org/doi/10.1021/acsomega.3c00100>.

¹H NMR, ¹³C NMR, and mass spectra and HPLC data of BCL, BHM, and BCD (PDF)

■ AUTHOR INFORMATION

Corresponding Authors

Anandarup Goswami – Department of Chemistry, School of Applied Science and Humanities, Vignan's Foundation for Science, Technology and Research (Deemed to be University), Guntur 522 213, India; orcid.org/0000-0003-4696-8247; Email: ananda1911@gmail.com

Naveen Mulakayala – SVAK Lifesciences, Hyderabad 500090 Telangana, India; orcid.org/0000-0002-5621-6455; Email: naveen071280@gmail.com

Authors

Guruswamy Vaddamanu – Department of Chemistry, School of Applied Science and Humanities, Vignan's Foundation for Science, Technology and Research (Deemed to be University), Guntur 522 213, India; SVAK Lifesciences, Hyderabad 500090 Telangana, India

N. Ravi Sekhar Reddy – SVAK Lifesciences, Hyderabad 500090 Telangana, India

Katam Reddy Vinod Kumar Reddy – SVAK Lifesciences, Hyderabad 500090 Telangana, India

Complete contact information is available at: <https://pubs.acs.org/doi/10.1021/acsomega.3c00100>

Author Contributions

CRedit Authorship Contribution Statement: **Guruswamy Vaddamanu**: experiments, analysis, study, methodology, validation, visualization, and writing—original draft. **N. Ravishekar Reddy** and **Katam Reddy Vinod Kumar Reddy**: project administration, supervision, and visualization. **Anandarup Goswami** and **Naveen Mulakayala**: writing—review and editing.

Notes

The authors declare no competing financial interest.

■ ACKNOWLEDGMENTS

We are thankful to SVAK Life Sciences and Vignan University for supporting us to conduct this work.

■ REFERENCES

- (1) Supady, A.; Zeiser, R. Baricitinib for patients with severe COVID-19-time to change the standard of care? *Lancet Respir. Med.* **2022**, *10*, 314–315.
- (2) Richardson, P.; Griffin, I.; Tucker, C.; Smith, D.; Oechsle, O.; Phelan, A.; Rawling, M.; Savory, E.; Stebbing, J. Baricitinib as potential treatment for 2019-nCoV acute respiratory disease. *Lancet* **2020**, *395*, e30–e31.
- (3) Stebbing, J.; Phelan, A.; Griffin, I.; Tucker, C.; Oechsle, O.; Smith, D.; Richardson, P. COVID-19: combining antiviral and anti-inflammatory treatments. *Lancet Infect. Dis.* **2020**, *20*, 400–402.
- (4) Phan, K.; Sebaratnam, D. F. JAK inhibitors for alopecia areata: a systematic review and meta-analysis. *J. Eur. Acad. Dermatol. Venereol.* **2019**, *33*, 850–856.
- (5) Kalil, A. C.; Patterson, T. F.; Mehta, A. K.; Tomashek, K. M.; Wolfe, C. R.; Ghazaryan, V.; Marconi, V. C.; Ruiz-Palacios, G. M.; Hsieh, L.; Kline, S.; Tapson, V.; Iovine, N. M.; Jain, M. K.; Sweeney, D. A.; El Sahly, H. M.; Branche, A. R.; Regalado Pineda, J.; Lye, D. C.; Sandkovsky, U.; Luetkemeyer, A. F.; Cohen, S. H.; Finberg, R. W.; Jackson, P. E. H.; Taiwo, B.; Paules, C. I.; Arguinchona, H.; Erdmann, N.; Ahuja, N.; Frank, M.; Oh, M. D.; Kim, E. S.; Tan, S. Y.; Mularski, R. A.; Nielsen, H.; Ponce, P. O.; Taylor, B. S.; Larson, L.; Roupahel, N. G.; Saklawi, Y.; Cantos, V. D.; Ko, E. R.; Engemann, J. J.; Amin, A. N.; Watanabe, M.; Billings, J.; Elie, M. C.; Davey, R. T.; Burgess, T. H.; Ferreira, J.; Green, M.; Makowski, M.; Cardoso, A.; de Bono, S.; Bonnett, T.; Proschan, M.; Deye, G. A.; Dempsey, W.; Nayak, S. U.; Dodd, L. E.; Beigel, J. H. Baricitinib plus Remdesivir for Hospitalized Adults with Covid-19. *N. Engl. J. Med.* **2021**, *384*, 795–807.
- (6) Huang, F.; Luo, H.; Gong, J.; Wang, D.; Hu, M.; Huang, W.; Fang, K.; Qin, X.; Qiu, X.; Yang, X.; Lu, F. Risk of Adverse Drug Events Observed with Baricitinib 2 mg Versus Baricitinib 4 mg Once Daily for the Treatment of Rheumatoid Arthritis: A Systematic Review and Meta-Analysis of Randomized Controlled Trials. *BioDrugs* **2018**, *32*, 415–423.
- (7) Teasdale, A.; Elder, D.; Harvey, J.; Spanhaak, S. *ICH Quality Guidelines*, Wiley, 2017.
- (8) Görög, S. The importance and the challenges of impurity profiling in modern pharmaceutical analysis. *TrAC, Trends Anal. Chem.* **2006**, *25*, 755–757.
- (9) International Conference on Harmonization of Technical Requirements for Registration of Pharmaceuticals for Human Use, ICH Q3A(R2) Impurities in New Drug Substances, 2006; Vol. 1–15.
- (10) Gorog, S. *Identification and Determination of Impurities in Drugs*; Elsevier: Amsterdam, 2000; Vol. 4, pp. 1–8.
- (11) Rodgers, J. D.; Shepard, S.; Li, Y.-L.; Zhou, J.; Liu, P.; Meloni, D.; Xia, M. Azetidine and cyclobutene derivatives as JAK inhibitors, WO 2009114512 A1, 2009.
- (12) Dasari, S. R.; Seelam, N.; Jayachandra, S.; Vadali, L. R.; Yerva, E. R.; Tondepur, S.; Gadakar, M. K. Synthesis and Characterization of Compounds Potentially Related to the Janus Kinase Inhibitor Baricitinib. *Russ. J. Org. Chem.* **2019**, *55*, 1569–1574.
- (13) Sadineni, R. K.; Rapolu, R. K.; Raju, V. V. N. K. V. P.; Srinivasu, S.; Malladi, S.; Mulakayala, N. Novel method for the synthesis of lenvatinib using 4-nitrophenyl cyclopropylcarbamate and their pharmaceutical salts. *Chem. Pap.* **2021**, *75*, 1475–1483.
- (14) Rapolu, R. K.; Arevelu, S.; Raju, V. V. N. K. V. P.; Navuluri, S.; Chavali, N.; Mulakayala, N. An Efficient Synthesis of Darunavir Substantially Free from Impurities: Synthesis and Characterization of Novel Impurities. *ChemistrySelect* **2019**, *4*, 4422.
- (15) Gudisela, M. R.; Bommu, P.; Navuluri, S.; Mulakayala, N. Synthesis and Characterization of Potential Impurities of Dolutegravir: A HIV Drug. *ChemistrySelect* **2018**, *3*, 7152.